Thermal bistability through coupled photonic resonances

Chinmay Khandekar[1] and Alejandro W. Rodriguez[1]
Princeton University, Princeton, NJ 08544, USA

We present a scheme for achieving thermal bistability based on the selective coupling of three optical resonances. This approach requires one of the resonant frequencies to be temperature dependent, which can occur in materials exhibiting strong thermo-optic effects. For illustration, we explore thermal bistability in two different passive systems, involving either a periodic array of Si ring resonators or parallel GaAs thin films separated by vacuum and exchanging heat in the near field. Such a scheme could prove useful for thermal memory devices operating with transition times $\lesssim$ hundreds of milliseconds.

Rapid progress in the synthesis and processing of materials at small lengthscales has created demand for understanding thermal phenomena in nanoscale systems.[1,2] Recent interest in harnessing excess heat that is readily available at the nanoscale has culminated in several proposed thermal devices[3] with various functionalities, including thermal rectifiers,[4] thermal memory,[5] thermal transistors,[6] phononic logic gates,[7] and phonon waveguides.[8]. In this paper, we propose a scheme to achieve thermal bistability based on the coupling between three or more optical resonances. Our approach complements and builds on recently proposed ideas[5,9–11] in several ways, described further below.

A thermal, bistable system can be used as a memory device that stores thermal information by maintaining the temperature of the system in one of two or more possible states. Realizing such temperature bistability requires a nonequilibrium thermal circuit supporting multiple steady states. Such a circuit was first proposed several years ago based on the concept of negative differential thermal resistance (NDTR), which relies on the ability to achieve heat flux rates between objects that decrease with increasing temperature differences. While first proposed in a model system consisting of a lattice of one-dimensional nonlinear mechanical oscillators,[5] recent implementations of NDTR have instead sought to exploit radiative energy transfer between slabs separated by nanometer gaps and heated to very high $\approx$ 1500K temperatures.[11,12]. Here, we propose a simple and experimentally feasible, all-optical scheme based on a system of three optical resonances that builds and expands on a recently proposed and related scheme which requires materials supporting metal-insulator phase-transitions.[9,10] Instead, our approach exploits common materials exhibiting strong thermo-optic effects and relies instead on thermal bistability induced by a resonant mechanism involving three optical resonances—microring cavities supporting travelling-wave resonances or polar–dielectric slabs supporting surface–propagating polaritonic resonances. This work extends previous studies of thermal rectification[4,13] and NDTR through vacuum[11] and also parallels recent ideas based on exotic non-volatile memory systems,[12,14,15] which have recently been proposed as viable alternatives to traditional electrostatic memory.[16,17]

Thermal bistability in triply resonant structures.— We begin by briefly describing the main mechanism behind the proposed thermal bistability scheme, leaving quantitative predictions for later. Consider a system of three thermal bodies, shown schematically in Fig. 1(a), two of which are maintained at constant temperatures T_h and T_c, with $T_h > T_c$, while the remaining body is thermally isolated from its surroundings and has variable temperature T_0. The hot and cold bodies exchange heat with the isolated body through flux rates J_h and J_c, respectively, leading to a net heat influx $J_t = J_h - J_c$ and a steady-state temperature satisfying (neglecting losses due to thermal conduction) $\rho c_p V \frac{\partial T_0}{\partial t} = J_t = 0$, where ρ, c_p, V are the density, specific heat capacity, and volume of the body, respectively. For typical heat transfer mechanisms such as conduction[18] or radiation,[19] the

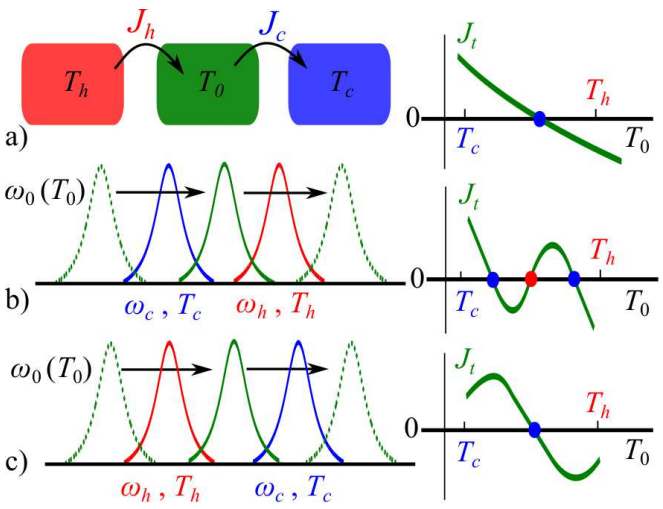

FIG. 1. (a) Schematic of three bodies in a nonequilibrium configuration of temperatures $T_h > T_0 > T_c$, where the hot and cold bodies are maintained at constant temperatures T_h and T_c, respectively, while the middle body has variable temperature T_0. The system reaches a steady state when the net heat exchanged $J_t = J_h - J_c = 0$ (blue dot), where J_h and J_c denote the heat flux rates between the hot and cold bodies and the middle body. When the main mechanism behind heat exchange is a resonant process mediated by photonic resonances in the bodies, the variation of $J_t(T_0)$ can become nonmonotonic. The schematics in (b,c) illustrate the expected dependence of J_t with T_0 when the relative frequencies of the resonators are either (b) $\omega_0(T_c) < \omega_c < \omega_h$ or (c) $\omega_0(T_c) < \omega_h < \omega_c$, where $\omega_0(T_0)$ depends linearly with T_0 due to thermoptic effects, illustrating the existence of multiple (stable or unstable) steady states.

heat flux between any two bodies increases with increasing temperature difference, leading to monotonic $J_t(T_0)$ and thereby giving rise to a single steady state, i.e. $J_t(T_0) = 0$, as illustrated in Fig. 1(a). As recently illustrated in Ref. 11, NDTR can be realized in the context of radiative heat transfer between bodies exhibiting significant thermo-optic effects: namely, by exploiting the monotonic increase in the frequency of planar resonances with increasing temperature. Here we extend this idea by considering a system of three bodies that support narrow and slightly detuned resonances of frequencies ω_j, with $j \in \{h, 0, c\}$. Consider a situation under which $T_0 = T_c$ and $\omega_0 < \omega_c < \omega_h$. As the temperature T_0 is increased from $T_c \to T_h$, ω_0 sweeps over the frequencies of both the hot and cold resonators, whose temperatures and frequencies are held fixed. As $\omega_0 \to \omega_c$, the two resonators exchange heat more effectively and hence experience larger overall heat loss, causing J_t to decrease considerably. As ω_0 moves past ω_c and approaches ω_h, J_t increases again due to increased coupling with the hot resonance, decreasing with increasing ω_0 as it moves past ω_h. Thus, if properly engineered, such a system can lead to three steady states, consistent with zero net heat exchange ($J_t = 0$). Such a situation is illustrated on the right half of Fig. 1(b), wherein the intermediate state (red dot) is unstable while the remaining two (blue dots) are stable, i.e. $\frac{\partial J_t}{\partial T_0} < 0$. If, on the other hand, the initial configuration is such that $\omega_0 < \omega_h < \omega_c$ when $T_0 = T_c$, similar arguments imply the existence of a single steady state, as illustrated in Fig. 1(c). While this NDTR scheme can be generalized to any system of resonances, below we consider and quantify the feasibility of observing thermal bistability using this scheme in realizations based on Si photonic resonators and GaAs thin films exchanging heat in the near field. Note that nonlinear thermo-optic effects in driven photonic resonators have been shown to lead to optical bistability[20], but their use as ultrafast optical memory devalues their potential as a slow thermal memory. In this work, we focus on passive systems in line with previous implementations of thermal memory, in which case no optical driving mechanisms are employed.

Ring resonators: We first focus on a system of Si ring resonators,[21,22] which exhibit both large thermo-optic coefficients and long-lived resonances at mid infrared wavelengths $\sim$ peak thermal wavelength $\lambda_T \sim 10\mu m$. In particular, we consider three one dimensional arrays of ring resonators shown in Fig. 2(a) with period Λ, two of which are maintained at fixed $T_h = 800$K (left) and $T_c = 300$K (right) while the middle one is suspended on insulating posts and has variable temperature T_0. We ignore the negligible interactions between adjacent rings along the array ensured by a sufficiently large Λ and obtain the flux rates by considering heat exchange for three coupled resonators shown schematically in the top inset of Fig. 2(a). Such a simplified system can be described via the temporal coupled-mode theory framework,[23–25] which provides accurate predictions while circumventing the need for numerically intensive calculations[26]. In this framework, the resonances are described by mode amplitudes a_j, normalized such that $|a_j|^2$ are mode energies,[26] and have frequencies ω_j and decay/loss rates γ_j, where $j = \{h, c, 0\}$. They are subject to thermal noise sources ξ_j described by delta-correlated, Gaussian noise terms satisfying $\langle \xi_j^*(\omega)\xi_j(\omega')\rangle = \delta(\omega - \omega')\Theta(\omega_j, T_j)$ where $\langle \cdots \rangle$ denotes the statistical ensemble average and $\Theta(\omega, T) = \hbar\omega/(e^{\frac{\hbar\omega}{k_B T}} - 1)$ is the Planck function. The three resonators are coupled to one another via coupling coefficients κ_h and κ_c, allowing heat to flow from the hot to the cold resonator as described by the following

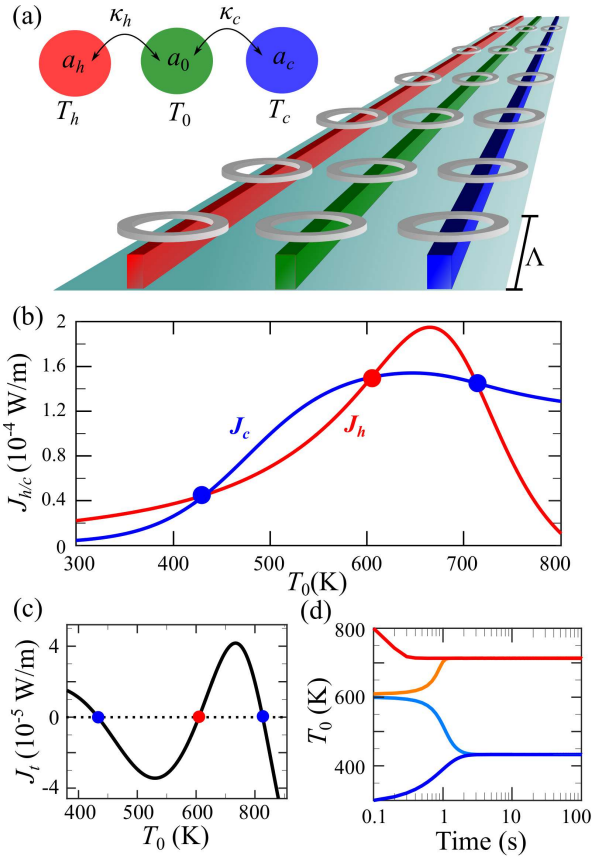

FIG. 2. (a) Schematic showing three arrays of Si ring resonators with periodicity $\Lambda = 1\mu$m, two of which are maintained at temperatures $T_h = 800K$ (red) and $T_c = 300K$ (blue), while the middle one (green) is suspended on insulating posts and has variable T_0. The heat-exchange rates per unit length between the hot/cold and intermediate arrays (unit cell shown schematically in the top inset) are J_h and J_c, respectively, plotted in (b) as a function of T_0 under suitable operating parameters (see text). (c) The nonmonotonicity in the net flux rate $J_t(T_0) = J_h - J_c$ indicates the existence of three steady states, two of which are stable (blue dots) and one unstable (red dot). (d) Temporal relaxation of the intermediate resonators starting from either T_h (red) or T_c (blue), along with the value of the unstable temperature point T_u, as they reach the steady-state temperatures, T_{s1} and T_{s2}.

coupled-mode equations:

$$\frac{da_h}{dt} = i\omega_h a_h - \gamma_h a_h + i\kappa_h a_0 + \sqrt{2\gamma_h}\xi_h \quad (1)$$

$$\frac{da_0}{dt} = i\omega_0(T_0) a_0 - \gamma_0 a_0 + i\kappa_h a_h + i\kappa_c a_c + \sqrt{2\gamma_0}\xi_0 \quad (2)$$

$$\frac{da_c}{dt} = i\omega_c a_c - \gamma_c a_c + i\kappa_c a_0 + \sqrt{2\gamma_c}\xi_c \quad (3)$$

Here, ω_0 depends on the local resonator temperature through the thermo-optic effect,[21] with $\omega_0(T_0) \approx \omega_0(T_c) + \frac{\omega_0}{n}\frac{\partial n}{\partial T_0}(T_0 - T_c)$, where n is the effective refractive index and $\frac{\partial n}{\partial T_0}$ the themo-optic coefficient of the resonator. It follows that the spectral flux densities associated with the coupled modes, $\Phi_{h/c} = 2\,\mathrm{Im}\{\kappa_{h/c}\}\langle a^*_{h/c} a_0\rangle$, are given by:

$$\Phi_h(\omega) = \frac{4\kappa_h^2\gamma_h(\kappa_c^2\gamma_c\Theta_{hc}(\omega) + \gamma_0|D_c(\omega)|^2\Theta_{h0}(\omega))}{|D_h(\omega)D_c(\omega)D_t(\omega)|^2} \quad (4)$$

$$\Phi_c(\omega) = \frac{4\kappa_c^2\gamma_c(\kappa_h^2\gamma_h\Theta_{hc}(\omega) + \gamma_0|D_h(\omega)|^2\Theta_{0c}(\omega))}{|D_h(\omega)D_c(\omega)D_t(\omega)|^2} \quad (5)$$

where $\Theta_{jk}(\omega) = \Theta(\omega, T_j) - \Theta(\omega, T_k)$ and $D_j(\omega) = i(\omega - \omega_j) + \gamma_j$, for $j, k \in \{h, 0, c\}$, and

$$D_t(\omega) = D_0(\omega) + \frac{\kappa_h^2}{D_h(\omega)} + \frac{\kappa_c^2}{D_c(\omega)}.$$

The net flux rates per unit length, $J_{h/c} = \frac{1}{\Lambda}\int \Phi_{h/c}(\omega)\frac{d\omega}{2\pi}$, are obtained by integrating over all frequencies.

As an illustration, we consider rings of radii $R_j = \frac{c}{n\omega_j}$ for $j \in \{h, 0, c\}$, designed to support resonances at $\omega_c = 3.62 \times 10^{14}$rad/s (5.2$\mu$m), $\omega_h = \omega_c + 7\gamma_c$, and $\omega_0(T_c) = \omega_c - 2\gamma_c$, with equal decay rates $\gamma_j = \omega_c/500$. Material properties are thermo-optic coefficient $\frac{\partial n}{\partial T} = 2\times10^{-4}K^{-1}$ and effective refractive index $n = 3.42$. With ring radii $R_j \sim 0.25\mu$m, lattice period $\Lambda = 1\mu$m is chosen to ignore the interactions between neighboring rings along the array and the arrays are placed such that the coupling rates $\kappa_h = 0.9\gamma_c$ and $\kappa_c = 2\gamma_c$. Figure 2(b) shows the flux rates J_h and J_c per unit length as a function of the temperature T_0 of the middle resonator. The net flux entering/leaving the ring J_t shown in Fig. 2(c) leads to two stable steady states at $T_{s1} = 413K$ and $T_{s2} = 700K$ (blue dots), along with an unstable state at $T_u = 600K$ (red dot). Here, we ignore radiative decay into the surroundings as well as conductive losses into the mechanically supporting structures. These extraneous channels of heat transfer can be suppressed by suspending the middle rings on thermally insulating posts to reduce conductive losses (see bottom schematic) while also operating under vacuum to eliminate conductive/convective heat transfer through air, as discussed in Ref. 27. Apart from stability against temperature perturbations, guaranteed here by large temperature gaps between steady states, robustness against flux perturbations will generally depend on the flux barrier and hence net magnitude of the flux rates $\sim \Theta(\omega, T)/Q$, guaranteed here by operating with large wavelengths and relatively small Q. Figure 2(d) illustrates the relaxation of T_0 from T_h, T_c, T_u^+, T_u^- to the nearest stable steady states T_{s1}, T_{s2}, assuming $V \sim 0.1\mu\mathrm{m}^3$ where V is the volume of the middle ring and the temperature-dependent values of c_p and ρ given in Ref. 28. While the relaxation time can be increased arbitrarily by setting the initial condition close to T_u, we estimate the characteristic "thermal memory" timescale as the maximum time it takes the middle ring to reach the stable steady states when its starting temperature is taken to be that of either the hot or cold resonators, which are 0.1s and 1s, respectively.

Compared to previous implementations based on phase-transition materials,[9,10] the transition times achieved here are of the same order of magnitude while the range of operating temperatures is wider by an order of magnitude. While the relaxation process can in principle be hastened by exploiting large thermo-optic coefficients and/or larger Q, thus decreasing the operating temperature range, the former are constrained by material choices while the latter lead to decreased flux rates. Aside from careful engineering of the coupling rates and resonator frequencies needed to achieve bistability, a thermal memory based on this setup requires good thermal insulation and suitable choice of materials exhibiting large thermo-optic coefficients for speed and improved stability (reliability).

Thin films: One possible way to increase the speed of such a thermal memory device is to exploit planar polaritonic materials, which offer enhanced heat flux rates owing to the large number of surface localized resonances they can support. In what follows, we consider one such example, shown schematically in Fig. 3(a), consisting of three GaAs thin films exchanging heat radiatively in the near field, where the hot and cold films are again held at fixed temperatures T_h and T_c, while the intermediate film is thermally insulated from its surroudings and hence described by a variable temperature T_0. Such a three-body planar configuration has been studied previously using scattering formulations, with the various flux rates obtained through straightforward calculation of the reflection/transmission matrices in this geometry,[29], as described in detail in Ref. 30. Here, we exploit this approach to consider a full calculation of the flux rates that includes thermo-optic effects in GaAs, obtained from Ref. 31, assuming operating temperatures $T_h = 1100$K and $T_c = 300$K, 200nm films, and vacuum gaps of $d_h = 48$nm and $d_c = 45$nm.

Figure 3(b) shows the computed flux rates per unit area, J_h and J_c, as a function of T_0, while the net flux entering/leaving the middle film J_t is shown in Fig. 3(c). As before, the thermo-optic induced NDTR results in two stable steady states at $T_{s1} = 430$K and $T_{s2} = 900K$ (blue dots) along with an unstable steady state at $T_u = 710K$ (red dot). Figure 3(d) illustrates the relaxation of T_0 from T_h, T_c, T_u^+, T_u^- to the nearest stable steady states, which is substantially decreased compared

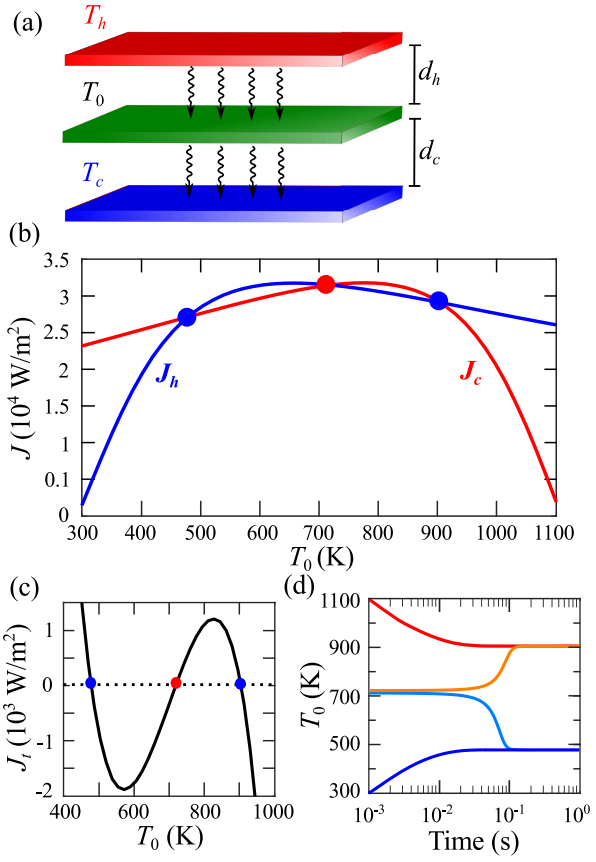

FIG. 3. (a) Schematic showing system of three planar GaAs thin films of equal thickness 200nm and separated by distances $d_h = 48$nm and $d_c = 45$nm, where the hot (red) and cold (blue) films are maintained at fixed temperatures, $T_h = 1100$K and $T_c = 300$K, while the middle film (green) is thermally insulated from the surroundings and has a variable T_0. (b) Heat flux rates per unit area, J_h and J_c, and (c) net flux rate $J_t = J_h - J_c$, as a function of T_0. The non-monotonicity in $J_t(T_0)$ results in three steady states, two of which are stable (blue dots) while the remaining one is unstable (red dot). (d) Temporal relaxation of the intermediate film starting from either T_h (red) or T_c (blue), along with the value of the unstable temperature point T_u, as it reaches the steady-state temperatures, T_{s1} and T_{s2}.

to ring resonators due to the significantly larger flux rates $\gtrsim 10^4$W/m^2 attained in this setup. Moreover, the characteristic timescale associated with such a relaxation, i.e. the maximum time it takes the middle film to reach a steady state when starting from T_h or T_c, is ≈ 0.1s and can be further decreased by going to smaller separations or smaller film thicknesses.

Note that a related NDTR-based mechanism was suggested in Ref. 11 in a system of two planar SiC plates. In that work, the heat flux between the two plates was shown to vary nonmonotonically at very high temperatures $T \sim 1500$K and small separations $d \sim 15$nm, in which case application of a constant (temperature independent) external flux leads to thermal bistability. Another recent work proposed a nanothermomechanical memory where NDTR is achieved at very high temperatures $T \sim 1100K$ by exploiting the nonmonotonic dependence of near field heat transfer on the separation between two planar slabs, as actuated by the thermal expansion of a mechanical support. The three-body system explored in this work relaxes some of these stringent operating conditions, allowing for a wide range of operating temperatures (steady state temperatures $\lesssim 1000$K) and flux rates. Furthermore, our proposed scheme also offers flexibility with respect to material choices in that it does not rely on phase-change materials[9] and could be realized with a wide range of materials exhibiting strong thermo-optic effects, such as chalcogenide glasses[32], silica[33], and silicon carbide[33], among many others. While thermal memory devices based on phase-transition materials offer a smaller operating temperature range (close to room temperature in case of vanadium dioxide[10]) and have also been shown to lead to multistability[34], our three-body scheme leads to wider temperature differences between the steady states, thereby guaranteeing stability against temperature and flux perturbations.

Concluding remarks: We demonstrated a simple scheme to realize temperature bistability in all-passive systems comprising multiple coupled resonant modes. We provided concrete predictions of expected operating conditions (including transition times of several hundred milliseconds) in realistic designs involving either suspended Si ring resonators or GaAs thin films. Since the underlying mechanism is very general and not restricted to the proposed implementations, one possible direction forward could be to explore other geometries such as nanobeam resonators[35], multilayered thin films[36], nanostructured materials[37,38] and different choices of materials[32,33], where one could potentially observe larger heat exchange. With rapidly advancing nanotechnology, the understanding of this and related thermal phenomena could be important for nanoscale heat management.

Acknowledgements: We would like to thank Riccardo Messina and Weiliang Jin for useful comments. This work was partially supported by the National Science Foundation under Grant no. DMR-1454836 and by the Princeton Center for Complex Materials, a MRSEC supported by NSF Grant DMR 1420541.

[1] David G Cahill, Wayne K Ford, Kenneth E Goodson, Gerald D Mahan, Arun Majumdar, Humphrey J Maris, Roberto Merlin, and Simon R Phillpot. Nanoscale thermal transport. *Journal of Applied Physics*, 93(2):793–818, 2003.

[2] Nianbei Li, Jie Ren, Lei Wang, Gang Zhang, Peter Hänggi, and Baowen Li. Colloquium: Phononics: Manipulating heat flow with electronic analogs and beyond. *Reviews of Modern Physics*, 84(3):1045, 2012.

[3] Bai Song, Anthony Fiorino, Edgar Meyhofer, and Pramod Reddy. Near-field radiative thermal transport: From theory to experiment. *AIP Advances*, 5(5):053503, 2015.

[4] Clayton R Otey, Wah Tung Lau, Shanhui Fan, et al. Thermal rectification through vacuum. *Physical Review Letters*, 104(15):154301, 2010.

[5] Lei Wang and Baowen Li. Thermal memory: a storage of

phononic information. *Physical review letters*, 101(26):267203, 2008.

[6] Philippe Ben-Abdallah and Svend-Age Biehs. Near-field thermal transistor. *Physical review letters*, 112(4):044301, 2014.

[7] Sophia R Sklan. Splash, pop, sizzle: Information processing with phononic computing. *AIP Advances*, 5(5):053302, 2015.

[8] Chih-Wei Chang, D Okawa, H Garcia, A Majumdar, and A Zettl. Nanotube phonon waveguide. *Physical review letters*, 99(4):045901, 2007.

[9] Viacheslav Kubytskyi, Svend-Age Biehs, and Philippe Ben-Abdallah. Radiative bistability and thermal memory. *Physical review letters*, 113(7):074301, 2014.

[10] Sergey A Dyakov, Jin Dai, Min Yan, and Min Qiu. Near field thermal memory based on radiative phase bistability of vo2. *Journal of Physics D: Applied Physics*, 48(30):305104, 2015.

[11] Linxiao Zhu, Clayton R Otey, and Shanhui Fan. Negative differential thermal conductance through vacuum. *Applied Physics Letters*, 100(4):044104, 2012.

[12] Mahmoud Elzouka and Sidy Ndao. Near-field nanothermomechanical memory. *Applied Physics Letters*, 105(24):243510, 2014.

[13] Zhen Chen, Carlaton Wong, Sean Lubner, Shannon Yee, John Miller, Wanyoung Jang, Corey Hardin, Anthony Fong, Javier E Garay, and Chris Dames. A photon thermal diode. *Nature communications*, 5, 2014.

[14] Elham Maghsoudi and Michael James Martin. Thermally actuated buckling beam memory: a non-volatile memory configuration for extreme space exploration environments. *Microsystem Technologies*, 22(5):1043–1053, 2016.

[15] Thomas Rueckes, Kyoungha Kim, Ernesto Joselevich, Greg Y Tseng, Chin-Li Cheung, and Charles M Lieber. Carbon nanotube-based nonvolatile random access memory for molecular computing. *science*, 289(5476):94–97, 2000.

[16] DN Nguyen, SM Guertin, GM Swift, and AH Johnston. Radiation effects on advanced flash memories. *IEEE Transactions on Nuclear Science*, 46(6):1744–1750, 1999.

[17] Marta Bagatin, Simone Gerardin, and Alessandro Paccagnella. Space and terrestrial radiation effects in flash memories. *Semiconductor Science and Technology*, 32(3):033003, 2017.

[18] JP Holman. Heat transfer, eighth si metric edition, 2001.

[19] Sergei M Rytov, Yurii A Kravtsov, and Valeryan I Tatarskii. Principles of statistical radiophysics 2. 1988.

[20] Libin Zhang, Yonghao Fei, Tongtong Cao, Yanmei Cao, Qingyang Xu, and Shaowu Chen. Multibistability and self-pulsation in nonlinear high-q silicon microring resonators considering thermo-optical effect. *Physical Review A*, 87(5):053805, 2013.

[21] Wim Bogaerts, Peter De Heyn, Thomas Van Vaerenbergh, Katrien De Vos, Shankar Kumar Selvaraja, Tom Claes, Pieter Dumon, Peter Bienstman, Dries Van Thourhout, and Roel Baets. Silicon microring resonators. *Laser & Photonics Reviews*, 6(1):47–73, 2012.

[22] Yang Xia, Ciyuan Qiu, Xuezhi Zhang, Weilu Gao, Jie Shu, and Qianfan Xu. Suspended si ring resonator for mid-ir application. *Optics letters*, 38(7):1122–1124, 2013.

[23] Wonjoo Suh, Zheng Wang, and Shanhui Fan. Temporal coupled-mode theory and the presence of non-orthogonal modes in lossless multimode cavities. *IEEE Journal of Quantum Electronics*, 40(10):1511–1518, 2004.

[24] Chinmay Khandekar, Zin Lin, and Alejandro W Rodriguez. Thermal radiation from optically driven kerr (χ (3)) photonic cavities. *Applied Physics Letters*, 106(15):151109, 2015.

[25] Linxiao Zhu, Sunil Sandhu, Clayton Otey, Shanhui Fan, Michael B Sinclair, and Ting Shan Luk. Temporal coupled mode theory for thermal emission from a single thermal emitter supporting either a single mode or an orthogonal set of modes. *Applied Physics Letters*, 102(10):103104, 2013.

[26] Hermann A. Haus. *Waves and field in optoelectronics*. Prentice Hall, 1984.

[27] Michael J Shaw, Michael R Watts, and Gregory N Nielson. Fabrication techniques for creating a thermally isolated tm-fpa (thermal microphotonic focal plane array). In *MOEMS-MEMS 2008 Micro and Nanofabrication*, pages 688308–688308. International Society for Optics and Photonics, 2008.

[28] Robert Hull. *Properties of crystalline silicon*. Number 20. IET, 1999.

[29] Riccardo Messina and Mauro Antezza. Three-body radiative heat transfer and casimir-lifshitz force out of thermal equilibrium for arbitrary bodies. *Physical Review A*, 89(5):052104, 2014.

[30] Mathieu Francoeur, M Pinar Mengüç, and Rodolphe Vaillon. Solution of near-field thermal radiation in one-dimensional layered media using dyadic green's functions and the scattering matrix method. *Journal of Quantitative Spectroscopy and Radiative Transfer*, 110(18):2002–2018, 2009.

[31] JS Blakemore. Semiconducting and other major properties of gallium arsenide. *Journal of Applied Physics*, 53(10):R123–R181, 1982.

[32] AB Seddon. Chalcogenide glasses: a review of their preparation, properties and applications. *Journal of Non-Crystalline Solids*, 184:44–50, 1995.

[33] Edward D Palik. *Handbook of optical constants of solids*, volume 3. Academic press, 1998.

[34] Kota Ito, Kazutaka Nishikawa, and Hideo Iizuka. Multilevel radiative thermal memory realized by the hysteretic metal-insulator transition of vanadium dioxide. *Applied Physics Letters*, 108(5):053507, 2016.

[35] Qimin Quan and Marko Loncar. Deterministic design of wavelength scale, ultra-high q photonic crystal nanobeam cavities. *Optics express*, 19(19):18529–18542, 2011.

[36] Svetlana V Boriskina, Jonathan K Tong, Yi Huang, Jiawei Zhou, Vazrik Chiloyan, and Gang Chen. Enhancement and tunability of near-field radiative heat transfer mediated by surface plasmon polaritons in thin plasmonic films. In *Photonics*, volume 2, pages 659–683. Multidisciplinary Digital Publishing Institute, 2015.

[37] Tengfei Luo and Gang Chen. Nanoscale heat transfer–from computation to experiment. *Physical Chemistry Chemical Physics*, 15(10):3389–3412, 2013.

[38] Andrew K Hafeli, Eden Rephaeli, Shanhui Fan, David G Cahill, and Thomas E Tiwald. Temperature dependence of surface phonon polaritons from a quartz grating. *Journal of Applied Physics*, 110(4):043517, 2011.